Parametric study of composite wind turbine blades

Kim, Taeseong; Branner, Kim; Hansen, Anders Melchior

Published in:
Proceedings of the Risø International Symposium on Materials Science

Publication date:
2011

Document Version
Publisher's PDF, also known as Version of record

PARAMETRIC STUDY OF COMPOSITE WIND TURBINE BLADES

T. Kim*, K. Branner*, and A. M. Hansen*

*Wind Energy Division, Risø National Laboratory for Sustainable Energy, Technical University of Denmark, 4000 Roskilde, Denmark

ABSTRACT

In this paper an anisotropic beam element for a composite wind turbine blades is developed. Eigenvalue analysis with the new beam element is conducted in order to understand its responses associated with the wind turbine performances. From the results of natural frequencies and mode shapes it is obvious that the anisotropic characteristics should not be ignored to obtain accurate results.

1. INTRODUCTION

For wind turbines blades, composite materials are widely used because they can reduce the total weight while retaining the structural properties and because they have good tailoring and fatigue life characteristics. The tailoring capability of the composite blade could be used to passively control the wind turbine response and results in a decrease of fatigue loads and the risk of flutter. It is shown in Luczak, Manzato, Peeters, Branner, Berring, and Kahsin (2011) that a typical wind turbine blade has very small couplings, but that these can be introduced easily by adding angled unidirectional layers. However, the aeroelastic codes in the wind energy fields such as HAWC2 still use the classical beam models. Therefore, it cannot be used to investigate the coupling effects of anisotropic materials.

In this paper a new beam element which is able to include anisotropic characteristics of a beam is developed and implemented into the structural part of the HAWC2.

2. METHODS

The classical Timoshenko beam element is currently used in HAWC2 by considering Finite Element Analysis (FEA). In order to compute the shape functions, static equilibrium equations are solved with geometric boundary conditions. The principle of virtual displacements is used to derive the element stiffness with the obtained shape functions. More detailed equations are

represented in Petersen (1990). However, the beam model in the current HAWC2 can generally not be extended to an anisotropic beam model because the shape functions do not necessarily capture the coupled motions. Therefore, a new beam element with new shape functions should be introduced to capture coupled behaviors. Fig. 1 shows a sketch of the coordinate system in HAWC2.

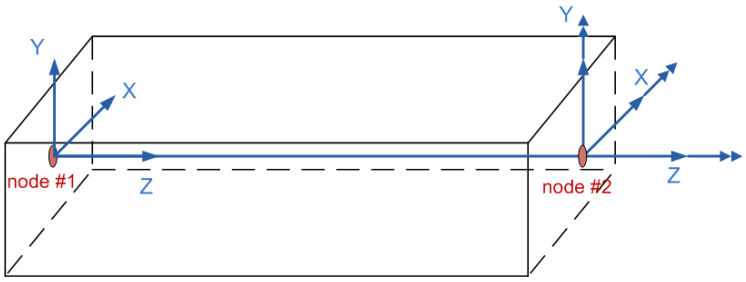

Fig.1: A sketch of the coordinate system

In order to compute the element stiffness and mass matrix, the elastic energy and the kinetic energy are considered.

2.1 Stiffness matrix. The elastic energy of the beam is defined as follows:

$$2U = \int_0^L \left(\varepsilon^T S \varepsilon\right) dz\,, \tag{1}$$

where S is the cross-sectional stiffness matrix defined by a diagonal matrix into the current HAWC2.

For the classical Timoshenko beam S is addressed by the diagonal matrix as follows:

$$S = diag\{k_x GA, \quad k_y GA, \quad EA, \quad EI_x, \quad EI_y, \quad GJ\}, \tag{2}$$

where k_x and k_y are shear factors related to forces in x and y directions, respectively.

In Eq. (1), ε the generalized strains of the Timoshenko beam are expressed as:

$$\begin{aligned} \{\varepsilon\}^T &= \{\varepsilon_x, \quad \varepsilon_y, \quad \varepsilon_z, \quad \kappa_x, \quad \kappa_y, \quad \kappa_z\} \\ &= \{u_x' - \theta_y, \quad -u_y' - \theta_x, \quad u_z', \quad \theta_x', \quad \theta_y', \quad \theta_z'\}, \end{aligned} \tag{3}$$

In FEA the displacement and rotation can be expressed by an interpolating polynomial in terms of generalized degrees of freedom as follows:

$$q(x) = \{u_x, \quad u_y, \quad u_z, \quad \theta_x, \quad \theta_y, \quad \theta_z\}^T = \underbrace{N(x)}_{6\times 6N_i} \underbrace{\alpha}_{6N_i\times 1}\,, \tag{4}$$

where N is the polynomial matrix in which, $\lfloor N \rfloor = \lfloor 1 \quad x \quad x^2 \quad \cdots \quad x^n \rfloor$ where n=1 for a linear polynomial, α are the generalized degrees of freedom, and N_i is the highest power in the polynomial + 1.

From the Eqs. (3) and (4) the generalized strain can be expanded in terms of a strain-displacement matrix and generalized degrees of freedom as follows:

$$\varepsilon = \underbrace{B(x)}_{6\times 6N_i}\underbrace{\alpha}_{6N_i\times 1}, \tag{5}$$

where B is the strain-displacement matrix which includes a polynomial matrix and its derivative terms as follows:

$$\underbrace{B(x)}_{6\times 6N_i} = B_0 N(x) + B_1 N'(x), \tag{6}$$

By substituting Eq. (5) into Eq. (1), the elastic energy of the beam can be illustrated as follows:

$$2U = \alpha^T \underbrace{\int_0^L \left(B^T S B\right) dz}_{D}\alpha, \tag{7}$$

In order to find α in Eq. (7) the boundary conditions at the beam ends are satisfied and the beam sections are in equilibrium which can be obtained when the total elastic energy is minimized. By applying boundary conditions the nodal degrees of freedom are obtained as follows:

$$\underbrace{d}_{12\times 1} = \underbrace{N_d}_{12\times 6N_i}\underbrace{\alpha}_{6N_i\times 1} = \begin{bmatrix} N_1 & N_2 \end{bmatrix}\begin{Bmatrix}\alpha_1\\ \alpha_2\end{Bmatrix}, \tag{8}$$

Here N_1 is a 12 by 12 matrix which is assumed to be invertible. Therefore, N_1 and N_2 become:

$$\underbrace{N_1}_{12\times 12} = \begin{bmatrix} I & 0\\ I & LI\end{bmatrix},\quad \underbrace{N_2}_{12\times(6N_i-12)} = \begin{bmatrix} 0 & 0 & \cdots & 0\\ L^2 I & L^3 I & \cdots & L^{N_i-1} I\end{bmatrix}, \tag{9}$$

where L is the length of the beam element.

From Eq. (8) α_1 can be rewritten as:

$$\alpha_1 = N_1^{-1}\left(d - N_2\alpha_2\right), \tag{10}$$

Therefore α can be expressed as follows:

$$\alpha = \begin{Bmatrix}\alpha_1\\ \alpha_2\end{Bmatrix} = \begin{bmatrix} N_1^{-1} & -N_1^{-1}N_2\\ 0 & I\end{bmatrix}\begin{Bmatrix} d\\ \alpha_2\end{Bmatrix}$$

$$\therefore \underbrace{\alpha}_{6N_i\times 1} = \underbrace{\begin{bmatrix}\underbrace{I}_{12\times 12}\\ \underbrace{0}_{(6N_i-12)\times 12}\end{bmatrix}}_{A_{\alpha 1}}\underbrace{\alpha_1}_{12\times 1} + \underbrace{\begin{bmatrix}\underbrace{0}_{12\times(6N_i-12)}\\ \underbrace{I}_{(6N_i-12)\times(6N_i-12)}\end{bmatrix}}_{A_{\alpha 2}}\underbrace{\alpha_2}_{(6N_i-12)\times 1} = \underbrace{A_{\alpha 1}}_{6N_i\times 12}\underbrace{\alpha_1}_{12\times 1} + \underbrace{A_{\alpha 2}}_{6N_i\times(6N_i-12)}\underbrace{\alpha_2}_{(6N_i-12)\times 1} \tag{11}$$

$$= A_{\alpha 1}N_1^{-1}d - A_{\alpha 1}N_1^{-1}N_2\alpha_2 + A_{\alpha 2}\alpha_2,$$

To compute α vector, the total energy minimization approach in terms of α_2, $\frac{dU}{d\alpha_2} = 0$, is considered. From Eqs. (7) and (11), the total elastic energy of the beam is obtained as follows:

$$U = \frac{1}{2}\underbrace{\left(d^T N_1^{-T} A_{\alpha 1}{}^T - \alpha_2{}^T N_2{}^T N_1^{-T} A_{\alpha 1}{}^T + \alpha_2{}^T A_{\alpha 2}{}^T\right)}_{\alpha^T} D \underbrace{\left(A_{\alpha 1} N_1^{-1} d - A_{\alpha 1} N_1^{-1} N_2 \alpha_2 + A_{\alpha 2}\alpha_2\right)}_{\alpha}, \tag{12}$$

Resulting from the total energy minimization, the α_2 vector is obtained as follows:

$$\begin{aligned}
&\frac{dU}{d\alpha_2} = 0 \\
&\therefore \underbrace{\left\{\left(N_2{}^T N_1^{-T} A_{\alpha 1}{}^T D A_{\alpha 1} N_1^{-1}\right) - \left(A_{\alpha 2}{}^T D A_{\alpha 1} N_1^{-1}\right)\right\}}_{P} d \\
&\quad = \underbrace{\left\{\left(N_2{}^T N_1^{-T} A_{\alpha 1}{}^T D A_{\alpha 1} N_1^{-1} N_2\right) - \left(A_{\alpha 2}{}^T D A_{\alpha 1} N_1^{-1} N_2\right) - \left(N_2{}^T N_1^{-T} A_{\alpha 1}{}^T D A_{\alpha 2}\right) + \left(A_{\alpha 2}{}^T D A_{\alpha 2}\right)\right\}}_{Q} \alpha_2 \\
&\therefore \alpha_2 = \underbrace{Q^{-1}}_{(6N_i-12)\times(6N_i-12)} \quad \underbrace{P}_{(6N_i-12)\times 12} \quad \underbrace{d}_{12\times 1},
\end{aligned} \tag{13}$$

By substituting Eq. (13) into Eq. (11), the α vector as a function of the nodal degrees of freedom is represented as follows:

$$\begin{aligned}
\alpha &= A_{\alpha 1} N_1^{-1} d - A_{\alpha 1} N_1^{-1} N_2 Q^{-1} P d + A_{\alpha 2} Q^{-1} P d \\
&= \left(A_{\alpha 1} N_1^{-1} - A_{\alpha 1} N_1^{-1} N_2 Q^{-1} P + A_{\alpha 2} Q^{-1} P\right) d \\
&= \underbrace{N_\alpha}_{6N_i\times 12} d,
\end{aligned} \tag{14}$$

Finally, the elastic energy of the beam is obtained in terms of nodal degrees of freedom by substituting Eq. (14) into Eq. (7) as follows:

$$\begin{aligned}
U &= \frac{1}{2} d^T N_\alpha{}^T \left[\int_0^L \left(B^T S B\right) dz\right] N_\alpha d \\
&= \frac{1}{2} d^T K d,
\end{aligned} \tag{15}$$

where K matrix, $K = N_\alpha{}^T \left[\int_0^L \left(B^T S B\right) dz\right] N_\alpha$, is the element stiffness matrix.

2.2 Mass matrix. The method to compute the element mass matrix is similar to the definition of the stiffness matrix. The element mass matrix is obtained from the kinetic energy as follows:

$$\begin{aligned}
T &= \frac{1}{2}\int_V \rho \dot{r}^T \dot{r} dV \\
&= \frac{1}{2}\int_0^L \dot{r}^T E \dot{r} dz,
\end{aligned} \tag{16}$$

where ρ, $\dot{r}$, V, and E are the mass density, velocity of the body, volume of body and the cross-sectional mass matrix, respectively.

By applying the same shape function as the stiffness matrix, Eq. (16) can be extended as follows:

$$T = \frac{1}{2}\dot{d}^T N_\alpha{}^T \left[\int_0^L \left(N(x)^T EN(x)\right)dz\right] N_\alpha \dot{d} = \frac{1}{2}\dot{d}^T M \dot{d}, \tag{17}$$

where M matrix, $M = N_\alpha{}^T \left[\int_0^L \left(N^T EN\right)dz\right] N_\alpha$, is the element mass matrix.

3. RESULTS

After implementing this new beam element into HAWC2, three different cases are investigated in order to validate the new beam model. The effect of using an anisotropic material is studied as well. Three different cases are considered for this study. Fig. 2 (a), (b), and (c) show a sketch of the considered cases. Table 1 shows the detailed structural properties and cross-sectional stiffness matrix for the first example. For Case 2 and Case 3, only sectional stiffness information is displayed in Table 2. More detailed information about the material properties and geometries are addressed in Yu (2007) and Hodges, Atilgan, Fulton, and Rehfield (1991).

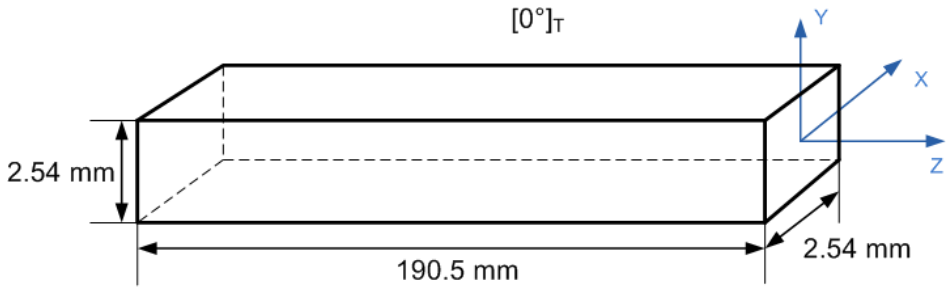

(a)

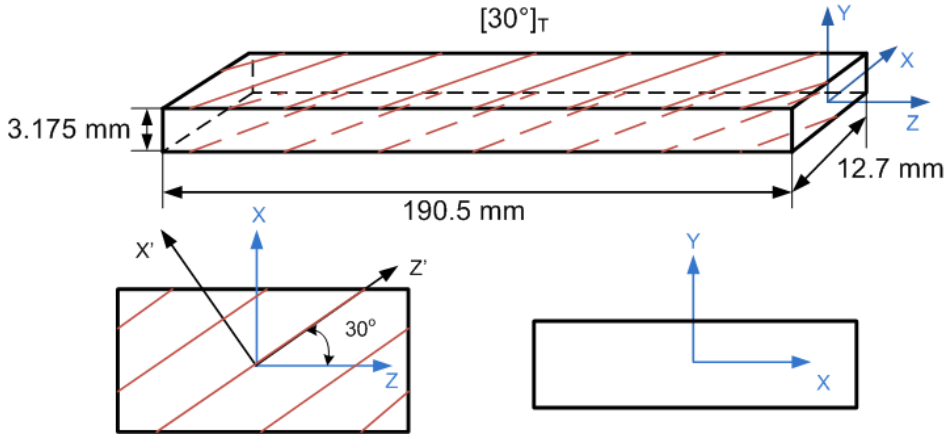

(b)

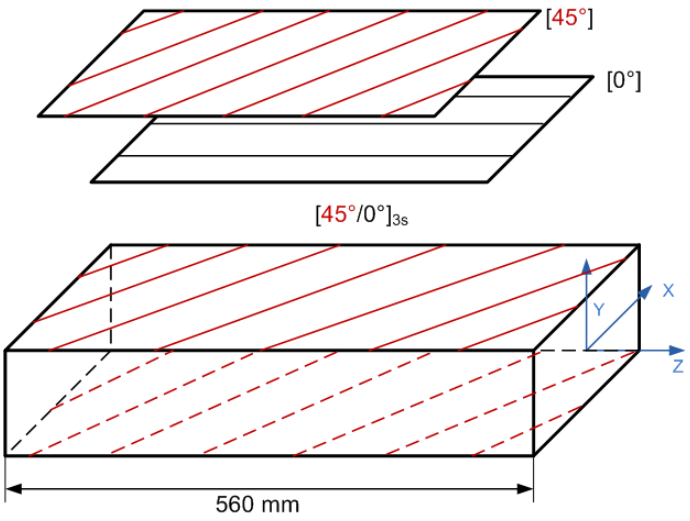

(c)

Fig.2. A sketch of considered cases. (a) Case1: $[0°]_T$ layup with arbitrary isotropic material, (b) Case2: $[30°]_T$ layup with Graphite/Epoxy, (c) Case3: $[45°/0°]_{3s}$ layups with Graphite/Epoxy.

Table 1. Structural properties of Case 1 (Blasques and Lazarov 2011)

Material	Arbitrary material
E_{11}, E_{22}, E_{33}	100 Pa
G_{12}, G_{13}, G_{23}	41.667 Pa
ν_{12}, ν_{13}, ν_{23}	0.2
ρ	1 kg/m^3
Width	0.1 m
Height	0.1 m
Length	7.5 m
Sectional stiffness of Case 1	
S_{11}, S_{22}	3.4899×10^{-1} (N)
S_{33}	1 (N)
S_{44}, S_{55}	8.3384×10^{-4} (N-m^2)
S_{66}	5.9084×10^{-4} (N-m^2)

Table 2. Sectional stiffness of Cases 2 and 3

Stiffness of Case 2 (Yu 2007)		Stiffness of Case 3 (Hodges et al. 1991)	
S_{11}	4.4702400×10^{5} (N)	S_{11}	4.1673312×10^{5} (N)
S_{13}	5.6667520×10^{5} (N)	S_{13}	-2.070544×10^{5} (N)
S_{22}	3.8404032×10^{4} (N)	S_{22}	3.0237504×10^{4} (N)
S_{33}	1.5861568×10^{6} (N)	S_{33}	3.6099968×10^{6} (N)
S_{44}	0.1313736×10^{1} (N-m^2)	S_{44}	5.314632×10^{-1} (N-m^2)
S_{46}	-9.225995×10^{-1} (N-m^2)	S_{46}	9.894628×10^{-2} (N-m^2)
S_{55}	1.1656606×10^{1}(N-m^2)	S_{55}	2.634072×10^{2}(N-m^2)
S_{66}	0.1454637×10^{1} (N-m^2)	S_{66}	3.584220×10^{-1} (N-m^2)

Case 1 is used for validating whether the new beam model is correctly implemented into HAWC2 or not. The other two cases are used for the comparisons between new HAWC2 computation with anisotropic material and the other existing results obtained from Yu (2007) and Hodges et al. (1991).

3.1 Natural frequencies and mode shapes. Eigenvalue analysis is performed for the three different cases. Table 3 shows the natural frequency comparisons of Case 1 between the new beam element before implementing HAWC2 and after implementation. They are completely identical. From this result, it may be concluded that the new beam element is successfully implemented into HAWC2.

Table 3. Natural frequency comparison of Case 1

Mode	New beam element only [Hz]	HAWC2 [Hz]
1	2.87262E-03	2.87262E-03
2	2.87262E-03	2.87262E-03
3	1.80466E-02	1.80466E-02
4	1.80466E-02	1.80466E-02
5	5.09409E-02	5.09409E-02
6	5.09409E-02	5.09409E-02
7	1.14752E-01	1.14752E-01

Table 4 shows the natural frequency comparisons between the other existing results and HAWC2 computation. The HAWC2 result shows good agreement with Yu (2007) and Hodges et al. (1991), respectively.

Table 4. Natural frequency comparisons of Cases 2 and 3

	Case 2	
Mode	HAWC2 [Hz]	Yu (2007) [Hz]
1 (flap-torsion)	52.5	52.6
2 (edge)	209.7	209.8
3 (flap-torsion)	326.1	326.3
4 (flap-torsion)	899.3	899.8
5 (edge)	1284.2	1284.9
6 (flap-torsion)	1660.9	1661.3

Mode	Case 3 HAWC2 [Hz]	Hodges et al. (1991) [Hz]
1 (flap-torsion)	4.66	4.66
2 (flap-torsion)	29.18	29.60
3 (flap-torsion)	81.57	84.89
4 (edge)	105.99	N/A
5 (flap-torsion)	113.35	113.43
6 (flap-torsion)	159.52	N/A

Small discrepancies in Cases 2 and 3 might occur due to converting the units from English to SI units and using different shape functions.

It is clear to see that flapwise bending-torsion and axial-edgewise deflections are coupled on the structure of Cases 2 and 3 from the Table 2. The coupling effects on the structure can be captured through the mode shape analyses. Fig. 3 shows the first 6 mode shapes of Case 2. From the mode 1, 3, 4, and 6 it is shown that the flap mode is coupled with the torsion mode.

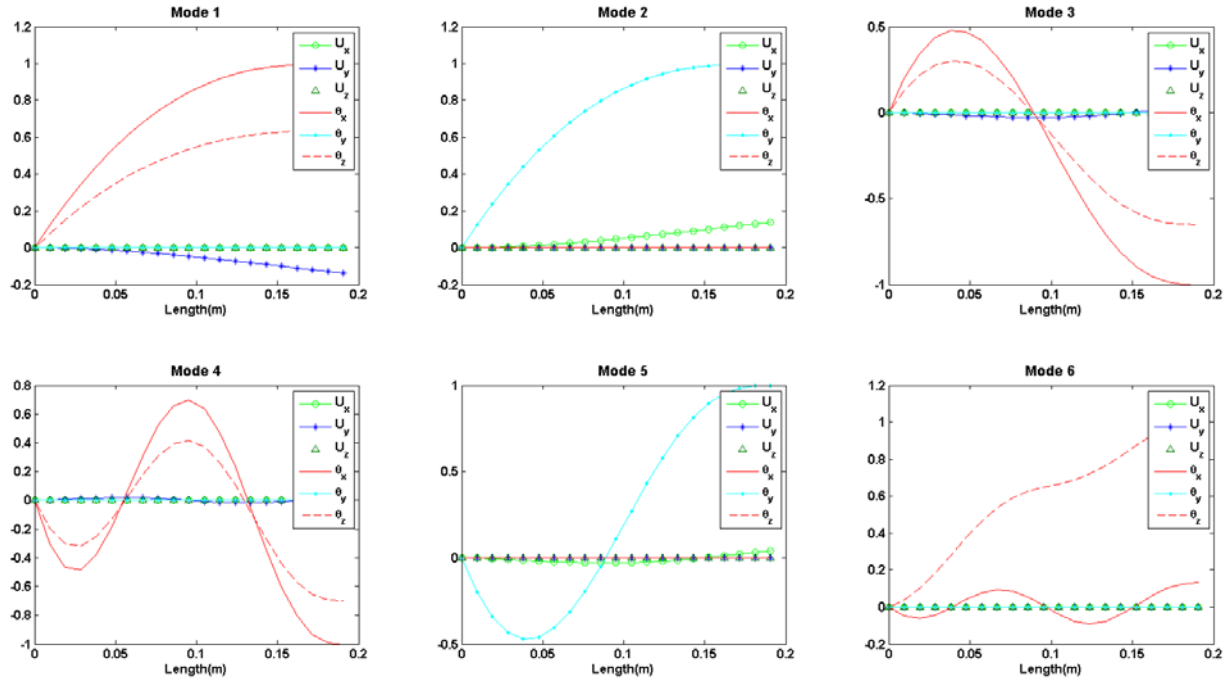

Fig. 3. First 6 mode shapes of Case 2 with anisotropic properties

Fig. 4 shows the first 6 mode shapes of Case 3. It is observed by mode 1, 2, 3, 5, and 6 that the flap mode is coupled with the torsion mode.

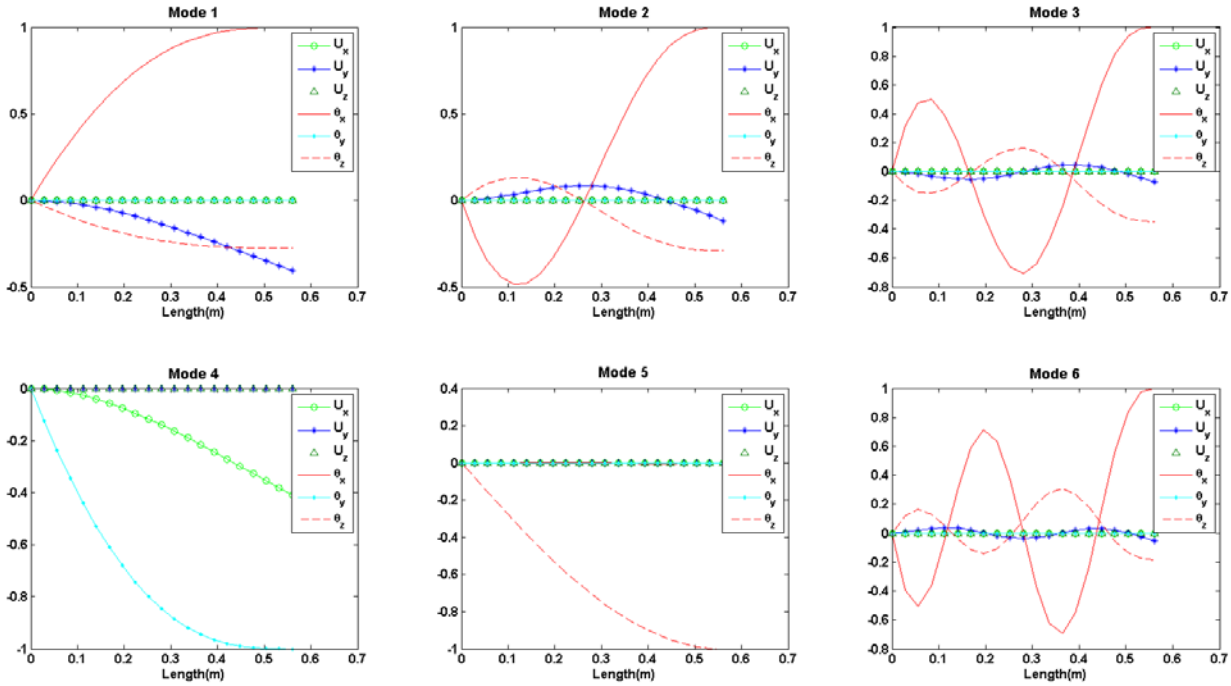

Fig. 4. First 6 mode shapes of Case 3 with anisotropic properties

From the above results of natural frequencies and mode shapes the new beam model can capture the physical behaviors of structural coupled characteristics.

An additional Eigenvalue analysis is performed with Cases 2 and 3 in order to investigate important physical differences between isotropic and anisotropic structures by using old versions (i.e. before implementing the new beam model) and new versions (i.e. after implementing the new beam model) of HAWC2. The old version of HACW2 considers the anisotropic characteristics produced by the shear center offset only (Petersen 1990; Larsen and Hansen 2007). However, its effect is ignored in this paper. Thus, it is assumed that the shear center is located at the center of the sections considered for both cases. In order to produce an isotropic structure, the off-diagonal terms in the anisotropic structural property are removed. Due to the mentioned assumption for the isotropic case the comparisons cannot offer equivalent conditions. However these comparisons may be helpful for understanding the physical differences between them.

Table 5 shows the natural frequency differences between the isotropic and the anisotropic model of Cases 2 and 3. The differences are obvious on the coupled modes because the isotropic model does not have the abilities to capture the coupling effects between modes.

Fig. 5 and 6 show the mode shapes of Cases 2 and 3 with an isotropic structure, respectively. As expected no coupled modes are observed.

Table 5. Natural frequency differences between isotropic and anisotropic model

HAWC2 simulation of Case 2			
Mode	Anisotropic [Hz]	Mode	Isotropic [Hz]
1 (flap-torsion)	52.5	1 (flap only)	70.5
2 (edge only)	209.7	2 (edge only)	210.0
3 (flap-torsion)	326.1	3 (flap only)	436.1
4 (flap-torsion)	899.3	4 (flap only)	1196.6
5 (edge only)	1284.2	5 (edge only)	1296.5
6 (flap-torsion)	1660.9	6 (torsion only)	1675.0
HAWC2 simulation of Case 3			
Mode	Anisotropic [Hz]	Mode	Isotropic [Hz]
1 (flap-torsion)	4.66	1 (flap only)	4.78
2 (flap-torsion)	29.18	2 (flap only)	29.97
3 (flap-torsion)	81.57	3 (flap only)	83.81
4 (edge only)	105.99	4 (edge only)	106.01
5 (flap-torsion)	113.35	5 (torsion only)	113.34
6 (flap-torsion)	159.52	6 (flap only)	163.95

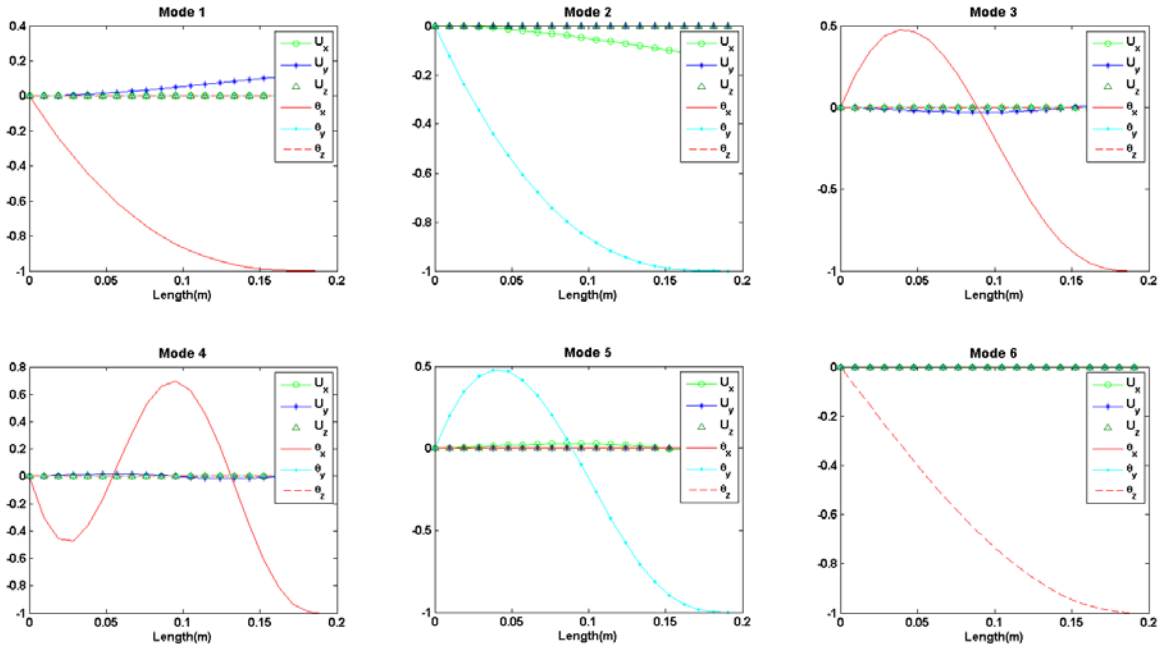

Fig. 5. First 6 mode shapes of Case 2 with isotropic properties

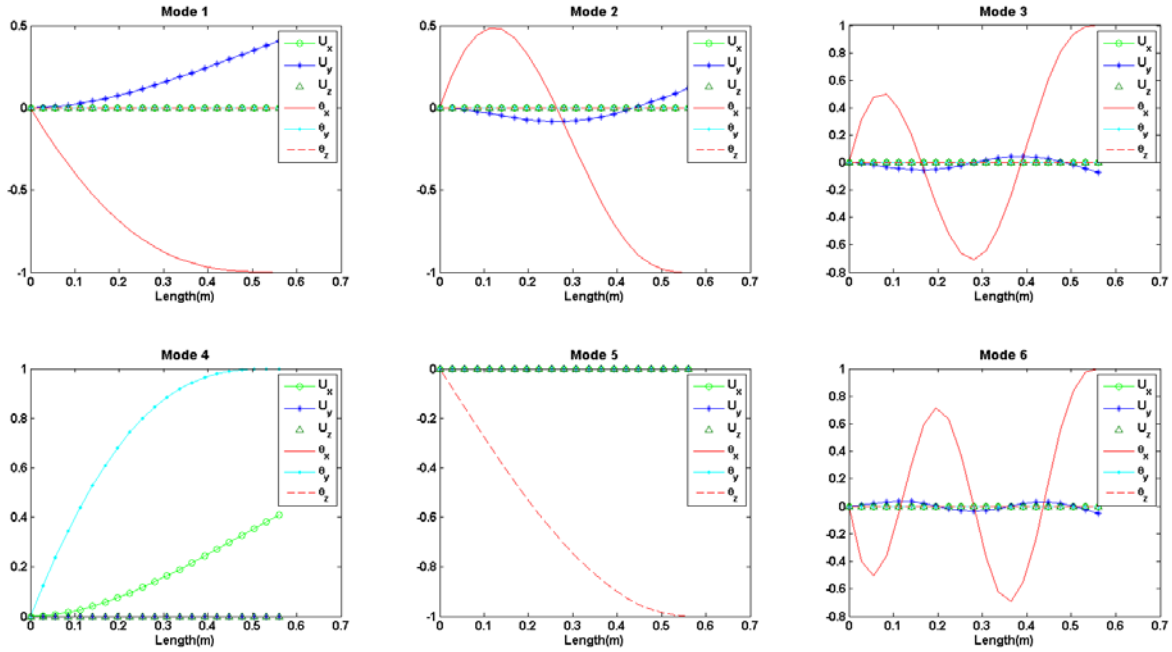

Fig. 6. First 6 mode shapes of Case 3 with isotropic properties

As we have investigated above there are differences between isotropic and anisotropic results for both the natural frequencies and mode shapes. Both are very important parameters when designing wind turbines. In that sense, the anisotropic behavior should be included in the relevant aeroelastic numerical tool if the blades have structural couplings.

4. CONCLUSIONS

In this paper, a new beam element which is able to consider the anisotropic behaviors is developed and implemented into HAWC2. Validations for the beam model and implementation are performed with 3 different cases. Eigenvalue analyses are performed. From the results the anisotropic characteristics show different behaviors compared to the isotropic ones. A new torsion mode, for instance, can be introduced by using bending-twist coupling of the anisotropic case. This additional effect may be used for developing new types of blades such as blades with less pitch control.

ACKNOWLEDGEMENTS

The work is partly supported by the Danish Energy Authority through the 2007 Energy Research Programme (EFP 2007). The supported EFP-project is titled “Anisotropic beam model for analysis and design of passive controlled wind turbine blades” and has journal no. 33033-0075. The support is gratefully acknowledged and highly appreciated.

REFERENCES

Blasques, J. P., and Lazarov, B. (2011). A Cross Section Analysis Tool for Anisotropic and Inhomogeneous Sections of Arbitrary Geometry. Risø-R-1785.

Hodges, D. H., Atilgan, A. R., Fulton, M. V., and Rehfield, L. W. (1991). Free-Vibration Anaysis of Composite Beams. Journal of the American Helicopter Society. 36(3), pp. 36-47.

Larsen, T.J., and Hansen, A.M. (2007). How 2 HAWC2, the user’s manual. Risø-R-1597(EN).

Luczak, M., Manzato, S., Peeters, B., Branner, K., Berring, P. & Kahsin, M. (2011). Dynamic

Investigation of Twist-bend Coupling in a Wind Turbine Blade. Journal of Theoretical and Applied Mechanics, 49(3)

Petersen , J.T. (1990). Kinematically Nonlinear Finite Element Model of a Horizontal Axis Wind Turbine- Part 1: Mathematical Model and Results. Ph.D. Thesis. Technical University of Denmark.

Yu, W. (2007). Efficient High-Fidelity Simulation of Multi-body Systems with Composite Dimensionally Reducible Components. Journal of the American Helicopter Society. 52(1), pp. 49-57.